Energy & Environmental Science

PAPER

View Article Online
View Journal

Cite this: DOI: 10.1039/c6ee00913a

CO_2 enabled process integration for the production of cellulosic ethanol using bionic liquids†

Jian Sun,[ab] N. V. S. N. Murthy Konda,[ac] Jian Shi,[ab] Ramakrishnan Parthasarathi,[ab] Tanmoy Dutta,[ab] Feng Xu,[ab] Corinne D. Scown,[abd] Blake A. Simmons[ab] and Seema Singh*[ab]

Received 26th March 2016,
Accepted 1st July 2016

DOI: 10.1039/c6ee00913a

www.rsc.org/ees

There is a clear and unmet need for a robust and affordable biomass conversion technology that can process a wide range of biomass feedstocks and produce high yields of fermentable sugars and biofuels with minimal intervention between unit operations. The lower microbial toxicity of recently-developed renewable ionic liquids (ILs), or bionic liquids (BILs), helps overcome the challenges associated with the integration of pretreatment with enzymatic saccharification and microbial fermentation. However, the most effective BILs known to date for biomass pretreatment form extremely basic pH solutions in the presence of water, and therefore require neutralization before the pH range is acceptable for the enzymes and microbes used to complete the biomass conversion process. Neutralization using acids creates unwanted secondary effects that are problematic for efficient and cost-effective biorefinery operations using either continuous or batch modes. We demonstrate a novel approach that addresses these challenges through the use of gaseous carbon dioxide to reversibly control the pH mismatch. This approach enables the realization of an integrated biomass conversion process that eliminates the need for intermediate washing and/or separation steps. A preliminary technoeconomic analysis indicates that this integrated approach could reduce production costs by 50–65% compared to previous IL biomass conversion methods studied.

Broader context

Ionic liquid (IL)-based pretreatment technology is known to be a very promising technology for the production of advanced biofuel and chemicals from lignocellulosic biomass. The relative toxicity, pH mismatch and recyclability of conventional ILs are some of the major hurdles that must be addressed in order to achieve a cost-effective IL-based biomass conversion technology. This work presents an innovative process that uses CO_2 as a reversible method of controlling pH that eliminates the need for separation and purification after biomass pretreatment. This approach achieves high yields of fermentable sugars and generates >80% of the theoretical yield of ethanol from glucose initially present in biomass using a renewable IL, cholinium lysinate, and commercially available enzyme mixtures and fermentation hosts. Based on a preliminary technoeconomic analysis, this approach achieves 50–65% reductions in terms of production costs relative to the conventional IL-based pretreatment and establishes a new paradigm for the production of biofuels from biomass using ILs, and addresses bio-/pH compatibility, process integration, and IL recycle challenges associated with those technologies.

Introduction

The substantial global supply of sustainable lignocellulosic biomass (*e.g.*, agricultural wastes, forestry wastes, dedicated energy crops, and organic municipal solid waste) makes it a vital feedstock for commercial-scale production of biofuels and renewable chemicals.[1,2] The efficient and affordable conversion of lignocellulosic biomass into fuels and chemicals is currently limited by, among other factors, its recalcitrance that inhibits efficient saccharification required to produce fermentable sugars.[3,4] To overcome this recalcitrance, and increase saccharification efficiency and yield, ionic liquid (IL) based pretreatment technologies are showing promise in meeting the desired key characteristics of biomass pretreatment.[5–7] The IL 1-ethyl-3-methylimidazolium acetate ($[C_2C_1Im][OAc]$) has been shown to be effective at decreasing the recalcitrance of both single and mixed lignocellulosic feedstocks, including softwoods and

[a] Deconstruction Division, Joint BioEnergy Institute, Emeryville, CA, USA. E-mail: seesing@sandia.gov
[b] Biological and Engineering Sciences Center, Sandia National Laboratories, Livermore, CA, USA
[c] Biological Systems Engineering Division, Lawrence Berkeley National Laboratory, Berkeley, CA, USA
[d] Energy Analysis and Environmental Impacts Division, Lawrence Berkeley National Laboratory, Berkeley, CA, USA

† Electronic supplementary information (ESI) available. See DOI: 10.1039/c6ee00913a

hardwoods,[8–10] with potential for producing renewable aromatics from lignin.[11] IL pretreatment using [C_2C_1Im][OAc] has been demonstrated at high solid loadings,[12,13] and recently scaled to larger volumes[14] and operated in continuous mode.[15]

Despite the effectiveness of [C_2C_1Im][OAc] and similar ILs in reducing the recalcitrance of lignocellulosic biomass, the inhibition of enzyme activity[16] and microbial toxicity[17] of these top performing ILs often require extensive water washes to remove residual IL from pretreated biomass prior to enzymatic hydrolysis and fermentation. As a result, the associated IL recycling and wastewater treatment costs create significant economic and process engineering challenges for the commercial scale-up of this technology.[18] To reduce water use, an integrated wash-free process using [C_2C_1Im][OAc] was recently developed,[19] where the pretreatment slurry was diluted with water to a final IL concentration of 10–20 wt% and directly hydrolyzed using a thermostable IL tolerant enzyme mixture, liberating 81.2% glucose and 87.4% xylose. This result provides the basis for developing a more economical IL pretreatment process, but requires specialized enzymes and is not compatible with the majority of the commercially available hydrolytic enzyme mixtures. In addition, downstream microbial fermentation is generally inhibited by the presence of residual ILs, and requires further separation and/or cleanup of the hydrolysate prior to fermentation.[20] Even with the recent discovery and expression/activation of efflux pumps in *Escherichia coli*[21] and the identification of strains of *Saccharomyces cerevisiae* with improved IL tolerance,[22,23] establishing an industrially relevant microbial host capable of withstanding the amounts of IL needed to decrease overall operating costs will require extensive research and development.

To address the economic and sustainability challenges associated with conventional ILs used for biomass pretreatment, a new generation of ILs containing ions derived from naturally occurring bases, acids and aldehydes from lignin and hemicellulose have recently emerged.[24–28] Despite these benefits, these "bionic liquids" (BILs) still operate, in general, at highly basic pH conditions and thus are not compatible with the commercially available cellulase and hemicellulase mixtures, nor are they compatible with microbial fermentation hosts that require neutral or slightly acidic conditions. To overcome this compatibility problem, a neutralization step is required before saccharification and fermentation. This is a common practice for other pretreatment technologies that use acids or bases. BILs have recently shown great potential,[24,28,29] but the higher cost of BILs relative to mineral acids necessitates that they are recycled (Fig. 1). A typical neutralization step leads to the formation of complex salts, from which there is no simple solution efficiently recovering and reusing ILs. This is a significant challenge that must be addressed to realize an integrated process and obligates exploration of clever approaches to overcome this present technology gap.

One potential solution to these challenges is to use a reversible and benign chemical input to adjust pH after pretreatment that enables process integration with saccharification and fermentation with no purification. Microbes produce

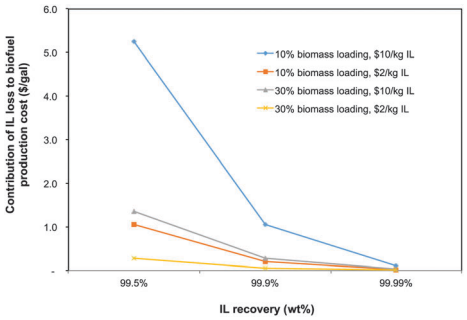

Fig. 1 Impact of IL recovery, IL price and biomass loading on biofuel production costs. The analysis is based on an industrial scale facility capable of processing 2000 dry MT per day biomass and producing around 60 million gallon fuel per year; a price range for ILs ($2 per kg to $10 per kg) is used in this analysis.

carbon dioxide (CO_2) during anaerobic fermentation, and the production of CO_2 at biorefineries has been considered to be a co-product.[30] It is known that certain ILs can capture high volumes of CO_2 under ambient or low-pressure conditions[31] that decrease pH by forming the corresponding carbonate salts. The process is reversible at elevated temperatures or by sparging nitrogen gas as previously reported for other ILs.[32,33]

To overcome the problems of IL loss in the current BIL process that would use commercially available enzyme mixtures and wild type fermentation hosts, we further tested the threshold of IL tolerance for cholinium lysinate ([Ch][Lys]) and other ILs. The use of CO_2 as a means of reversibly switching pH after pretreatment in order to develop an integrated process with minimal IL losses addresses several challenges with conventional pH adjustment, such as acid neutralization, and eliminates salt formation. The pretreated biomass generates high ethanol yields using wild type yeast (*S. cerevisiae*) in the presence of [Ch][Lys]. Recovery and recycle of the [Ch][Lys] was demonstrated and this approach shows significant potential to resolve several of the most significant obstacles towards the realization of an efficient, integrated, affordable and scalable IL conversion technology suitable for deployment at a biorefinery and opens the door to a new approach to biomass conversion into renewable biofuels and chemicals.

Toxicity comparison of ILs and tolerance threshold of fermentation host for [Ch][Lys]

Since [Ch][Lys] is known to be biocompatible,[26] we carried out the toxicity tolerance at even higher concentration to understand the upper limit of IL amount that could be employed in this integrated process. To identify the maximum amount of [Ch][Lys] that could be tolerated by the fermentation host, we tested the growth of wild type yeast strain with [Ch][Lys] concentration varying from 0, 10 and 20 wt%. In [Ch][Lys] concentrations of up to 10 wt%, *S. cerevisiae* showed no inhibition (Fig. 2a). These results indicate that [Ch][Lys] is intrinsically less toxic to this strain of *S. cerevisiae* BY4741.

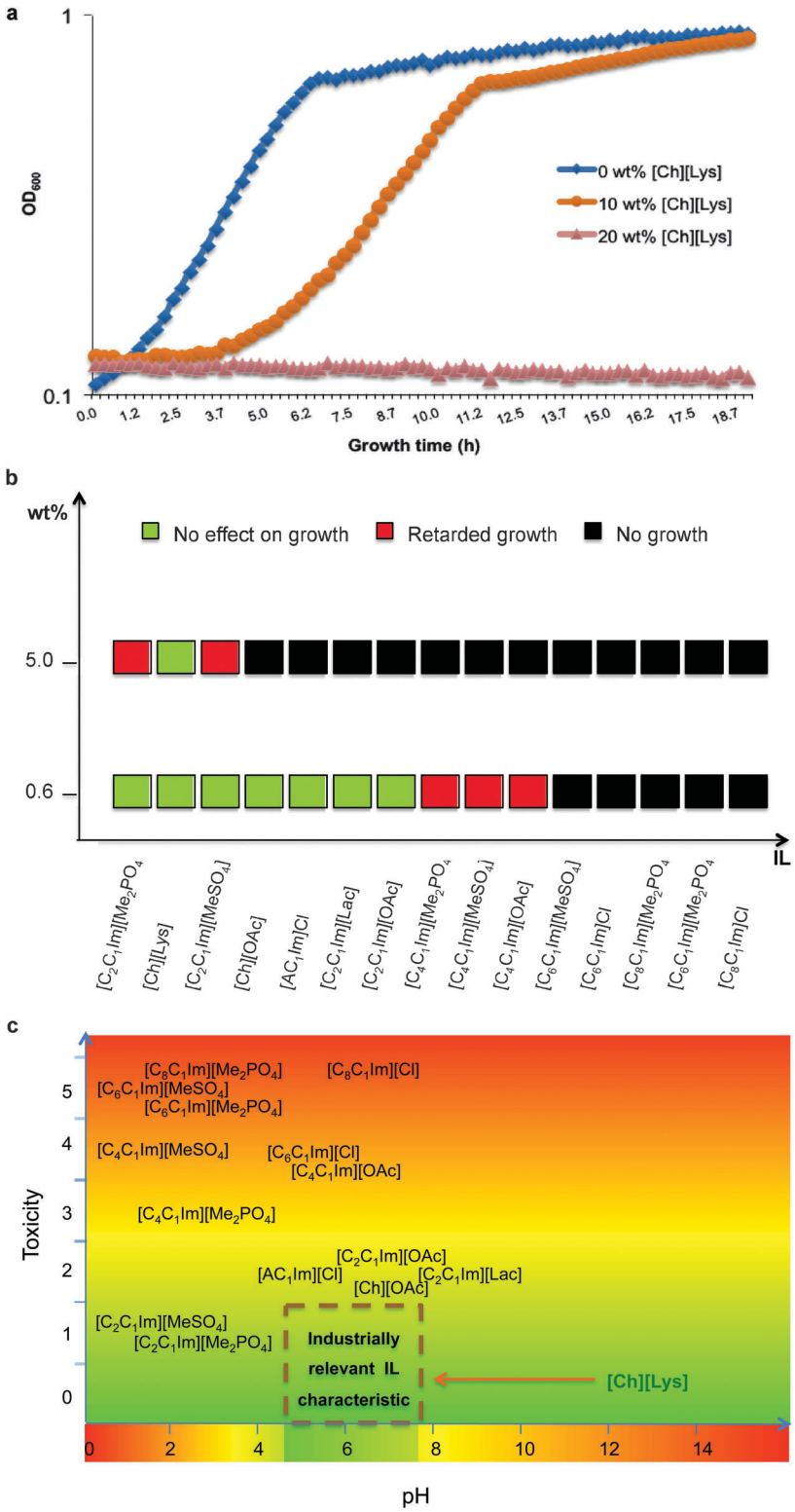

Fig. 2 Screening of Ionic liquid for the biocompatibility with *Saccharomyces cerevisiae* (a and b), and the relationship between pH and toxicity of ILs (c). The extent of cholinium lysinate toxicity is examined in (a) and the toxicity for various ILs are displayed in (b). Toxicity data is derived from the observed growth inhibition curves (see Fig. S1, ESI†) and displayed using a scale that ranges from black (very toxic), red (mildly toxic) to green (nontoxic).

We further tested the biocompatibility of a suite of other ILs to see whether any other IL or BIL could be employed in a similar fashion as [Ch][Lys] for the integrated process. The goal was to map the toxicity and pH to understand correlation and identification of ILs exhibiting both the compatibility and neutral pH characteristics helpful for establishing integrated

process, we carried out toxicity screens of 15 ILs including [Ch][Lys], cholinium acetate ([Ch][OAc]) and $[C_2C_1Im][OAc]$, which are some of the ILs previously shown to be effective at pretreating lignocellulosic biomass,[34–41] on *S. cerevisiae* strain BY4741 at IL concentrations of 0.6 and 5 wt% (for this purpose hydrochloric acid was used to neutralize the IL solution to pH 7). To resolve growth curves in different ILs and for clarity, the growth curve data is presented in pinwheel format (Fig S1, ESI†). The cytotoxicity indicator for various ILs tested are shown in Fig. 2b. At low concentration of IL (0.6 wt%), seven ILs such as 1-ethyl-3-methylimidazolium dimethylphosphate ($[C_2C_1Im][Me_2PO_4]$), [Ch][Lys], 1-ethyl-3-methylimidazolium methyl sulfate ($[C_2C_1Im][MeSO_4]$), [Ch][OAc], 1-alkyl-3-methylimidazolium chloride ($[AC_1Im][Cl]$), 1-ethyl-3-methylimidazolium lactate ($[C_2C_1Im][Lac]$) and ($[C_2C_1Im][OAc]$) show no toxicity to the growth (Fig. 2b). However, at higher concentration of 5 wt%, the *S. cerevisiae* growth was significantly inhibited for most of the ILs studied (Fig. 2b) except [Ch][Lys].

For an industrially relevant integrated conversion technology, the IL needs to have low microbial and enzymatic toxicity, high pretreatment efficiency and a mildly acidic to near neutral pH range ~4.5–7.5 for saccharification and fermentation. Comparison of [Ch][Lys] with $[C_2C_1Im][OAc]$ and their compatibility with commercial enzyme mixtures, in this case Novozymes Cellic® CTec2 and HTec2 (9 : 1, v/v), with the pH of the IL solution adjusted to 5.0 using hydrochloric acid are shown (Fig. S2, ESI†). When exposed to increasing levels of $[C_2C_1Im][OAc]$ (0, 5, 10, 20, 30 and 40 wt%), the relative activities of enzymes (in terms of sugar yield from enzymatic hydrolysis of microcrystalline cellulose) rapidly decline. At 5 wt% $[C_2C_1Im][OAc]$, the relative activity is only 47% of the no IL control; while only 30% activity remains at 10 wt% $[C_2C_1Im][OAc]$. However, [Ch][Lys] shows much less negative impact at these concentrations, with almost 70% and 50% of original enzyme activity at 5 and 10 wt% [Ch][Lys], respectively.

For comparison, the relationship between pH and toxicity of the fifteen ILs examined in this study are mapped in Fig. 2c. This map indicates that [Ch][Lys], $[C_2C_1Im][MeSO_4]$ and $[C_2C_1Im][Me_2PO_4]$ are the three low toxic ILs among the ILs investigated, but all of them have one major problem in that the pH of the IL is either too high or too low to maintain activity of commercial saccharolytic enzyme mixtures. Even so, [Ch][Lys] still has some very desirable attributes and thus was chosen for further investigation.

Exploiting chemistry of CO_2 and [Ch][Lys] for reversible pH adjustment

To enable integrated lignocellulosic biomass conversion using [Ch][Lys], the pH of the pretreatment slurry must be lowered to a range suitable for commercially available enzymes and microbes. The problems associated with the use of mineral/organic acids for pH adjustment favor the use of a volatile and easily reversible acidification agent, such as CO_2.[42] As a basic IL, [Ch][Lys] is highly effective in capturing CO_2 compared to imidazolium based ILs.[43] However, the efficiency of CO_2 capture for [Ch][Lys] is not understood or demonstrated in the presence of water. We therefore investigated the feasibility and reversibility of pH adjustment using CO_2 for an integrated pretreatment process technology using [Ch][Lys].

Interaction of CO_2 with amine containing molecules can proceed by either carbamate or carbamic acid reaction pathways.[44] In the presence of water, the CO_2 absorption by [Ch][Lys] is expected to proceed *via* the bicarbonate pathway. One or two CO_2 molecules can bind to the amine groups present in the lysinate anion forming carbonic acid and in turn lowering the pH (Fig. 3a). This interaction between aqueous solutions of [Ch][Lys], representative of the conditions present after biomass pretreatment, with CO_2 was evaluated using hybrid Density Functional Theory (DFT) based quantum chemistry approaches (Fig. 3b). The higher basicity of [Ch][Lys] is due to the unprotonated side chain amine group (Fig. 3a, red). The side chain amine group of $[Lys]^-$ forms hydrogen bonds with the hydroxyl group of $[Ch]^+$ (Fig. 3a). As shown (Fig. 3a), the interactions between water and side chain amines form a cyclic hydrogen-bonding network to bridge the cation and anion of [Ch][Lys]. The optimized structure obtained from our DFT calculations indicates that the side chain amine becomes a protonated amine when interacting with CO_2 in the presence of water.[45] The corresponding interactions were verified by nuclear magnetic resonance (NMR) analysis that shows multiple peaks in the range of 160–185 ppm in ^{13}C-NMR spectrum (Fig. S3, ESI†). Calculated acidity values of these IL–water–CO_2 complexes show a clear trend that CO_2 interactions with aqueous solutions of [Ch][Lys] increase the acidity and thereby decrease the pH (Table S1, ESI†). The computed nucleophilic attack (f_k^-) values of nitrogen atom in terminal and side chain groups are in good agreement with the observed trend in increasing acidity of the IL–water–CO_2 complexes (Fig. 3c). Due to the local charge distribution of the amine groups in [Ch][Lys] with CO_2 and corresponding interactions with H_2O, driving the molecular control of changing the pH, indicates that the presence of CO_2 is a reversible chemical trigger capable of reducing pH.

To validate our theoretical results and justify the selection of CO_2 as a practical means for pH adjustment, we designed experiments to optimize the conditions in water at room temperature. Fig. 4a shows that as predicted the pH indeed drops as a function of CO_2 pressure (0–2.4 MPa) for four different [Ch][Lys] concentrations (0, 5, 10 and 20 wt%). As CO_2 pressure is increased from 0 to 0.1 MPa, the pH values of all [Ch][Lys] solutions decreases sharply from a pH of ~12 to pH of 7–9. Further increase in CO_2 pressure led to increased lowering of the solution pH. For 20 wt% [Ch][Lys], a pH value of 7.2 was obtained at a CO_2 pressure of ~2 MPa. However, only 0.7 MPa CO_2 pressure is needed to drop the pH of 10 wt% [Ch][Lys] to a value of 7.1, and 0.1 MPa lowers the pH of the 5 wt% [Ch][Lys] to 6.9, which is similar to or lower than the typical pressure deployed for carbonating a can of soda.[46] In the case with no [Ch][Lys] present, the pH of water dropped quickly from around 7 to 3.7 as a function of increasing CO_2 pressure, which is caused by the formation of

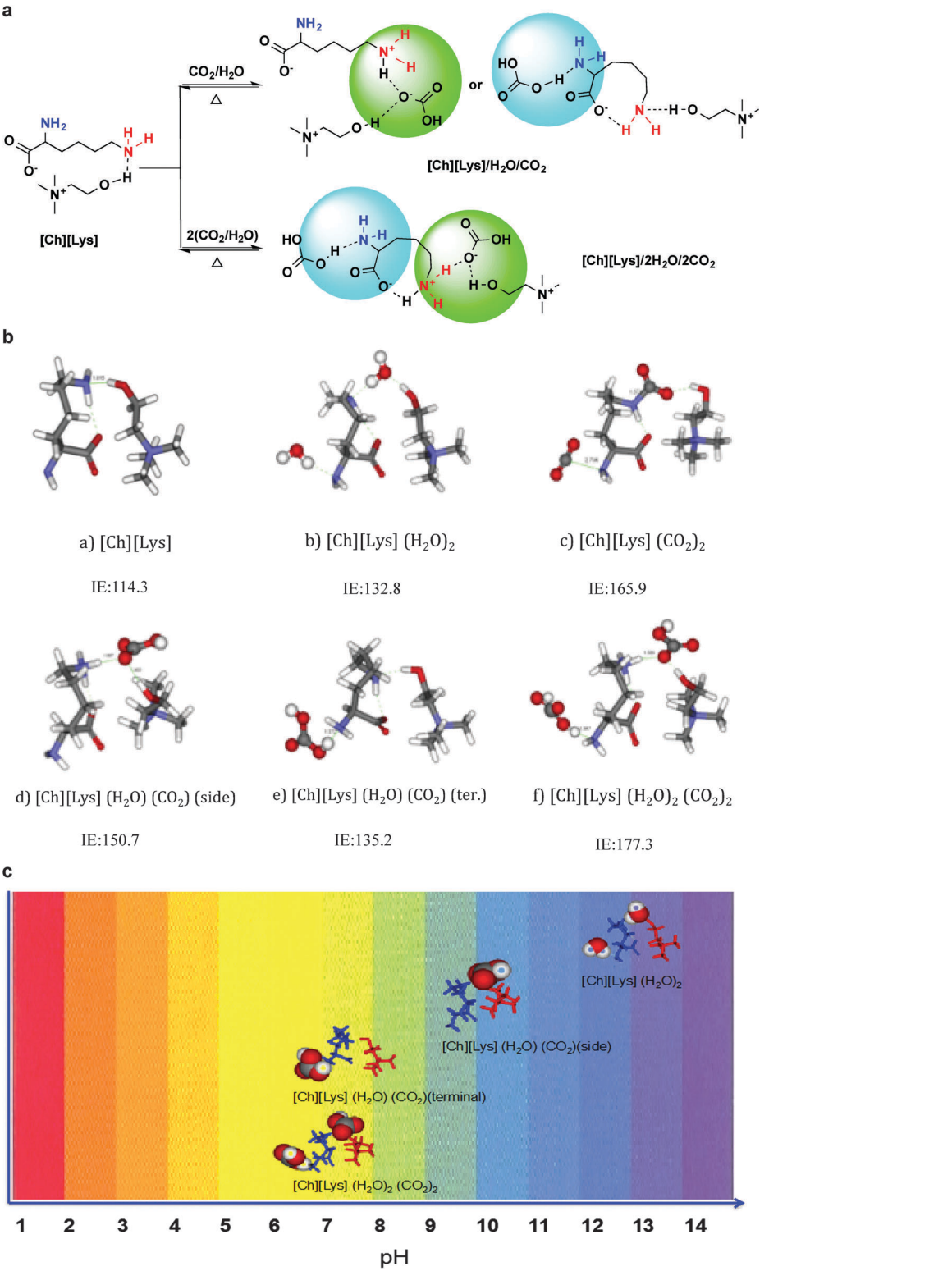

Fig. 3 Schematic of reversible CO_2-induced pH tuning for [Ch][Lys] (a), calculated interaction energy (IE in kcal mol^{-1}) profiles and optimized structures (in Å) of species for [Ch][Lys] *via* the CO_2 mediated pH shifts in the presence of H_2O (b), and molecular structure and calculated acidity of [Ch][Lys]/CO_2/water system (c).

carbonic acid. Based on this result, the carbonic acid formed during the integrated saccharification and fermentation process can further drop the pH value of the IL system. The pH obtained in the system by carbonation can support yeast growth as previous work has shown that *S. cerevisiae* is able to grow at a pH below 8.[47–49] Although we did not perform

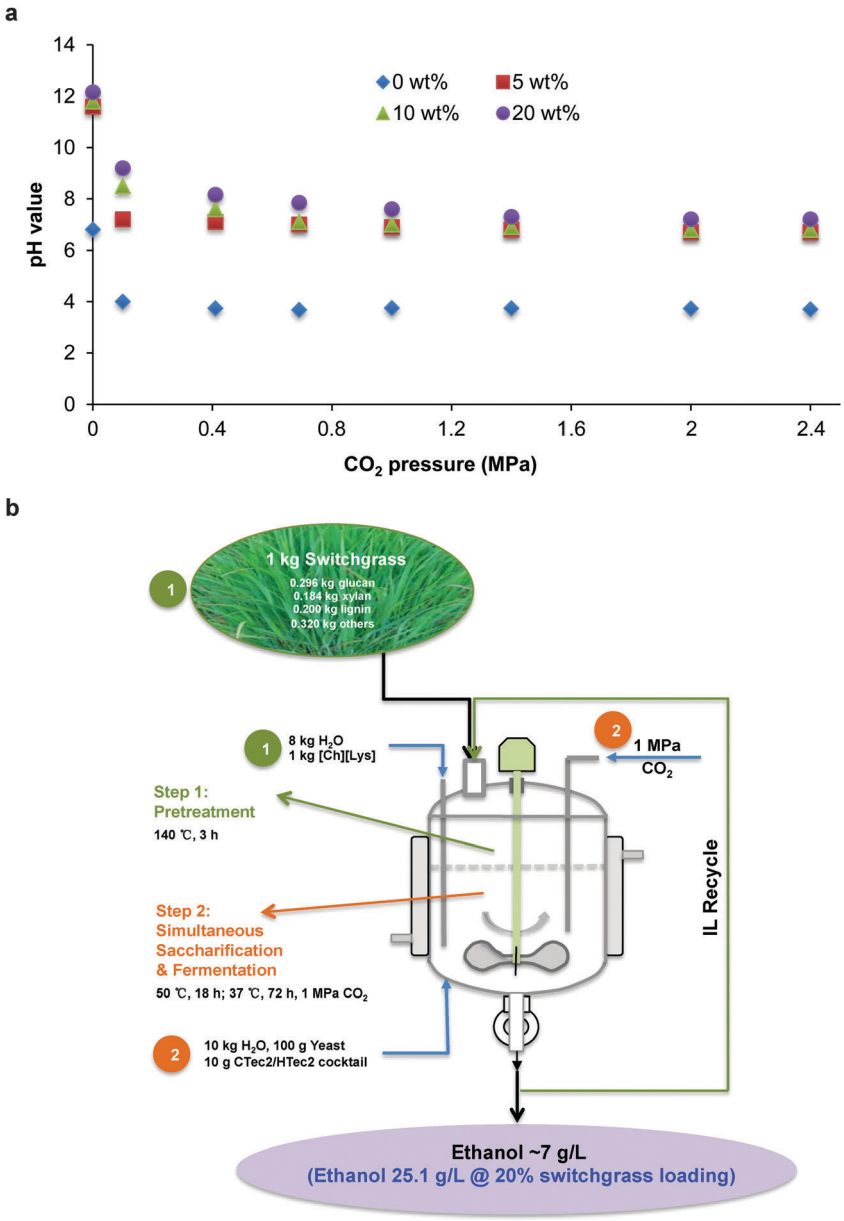

Fig. 4 Effect of CO_2 pressure on the pH adjustment of [Ch][Lys]/H_2O system (a), and ethanol production from switchgrass *via* CO_2 enabled integrated process using commercial enzymes and wild type yeast (b). In (a), [Ch][Lys] concentrations in water are 0, 5, 10 and 20 wt%, respectively; experiments were operated at 20 °C for 1 h.

in situ pH measurements due to the volume limitation of our reaction system for a pH probe, the high ethanol fermentation yield obtained in this work suggests that the pH value was maintained low enough for both enzyme and yeast activity.

Although the use of acids for pH adjustment is problematic for IL reuse and the focus of this work was to explore other alternative approach for pH adjustment, we examined the use of mineral and organic acids for the pH adjustment and compared the efficiencies of mineral acids and CO_2 approach. Out of seven acids tested, hydrochloric acid, sulfuric acid and citric acids were the only acids that enabled sugar production over 50% (Fig. S4, ESI†).

Integrated pretreatment, saccharification and fermentation

The reversible feature of CO_2–[Ch][Lys]–H_2O complex provides an unique opportunity for using CO_2 as a cheap, non-toxic, and volatile agent to adjust the pH and thus enable a new and integrated pretreatment and saccharification process using biocompatible IL and CO_2 without the need for special IL tolerant enzyme mixtures. Compared with the conventional water wash process (Fig. S7, ESI†) and JTherm based process[19] (Fig. S8, ESI†), the present work depicts a new IL conversion technology configuration (Fig. S9, ESI†), in which: (1) [Ch][Lys] was the IL used: (2) commercial enzyme mixtures was used for saccharification;

(3) CO_2 was used for reversible pH adjustment; (4) lignin separation through centrifugation; and (5) recycling of IL.

Results from a side-by-side comparison of the glucose and xylose yields liberated from switchgrass during pretreatment and saccharification for each of the three process scenarios (water wash, JTherm, and integrated) is reported in Fig. 6a. The CO_2 adjusted pH and [Ch][Lys] based integrated process achieved 87% glucose and 40% xylose yields after 72 h saccharification, which in terms of glucose yield is comparable to that of the conventional IL water-wash process and higher than the JTherm process. The result in the absence of [Ch][Lys] was better than that in the presence of [Ch][Lys] as we did not adjust the pH in the case where the IL was added (pH $\sim$ 12). Also the sugar yield from the CO_2 and [Ch][Lys] based integrated process was higher than that obtained by using HCl for pH adjustment (Fig. S4, ESI†).

In order to reduce the process complexity and improve overall process economics, using aqueous IL as a pretreatment medium is more favored over the use of anhydrous IL.[50] Recent studies have demonstrated that lower IL concentrations (10–50 wt%) in water may also be effective in pretreating biomass with certain ILs.[50] Using IL–H_2O mixture for biomass pretreatment offers many advantages such as lower viscosity, lower energy inputs and costs, and elimination of the dilution of pretreatment slurry for saccharification and dehydration of saccharification hydrolysate for IL recycle.[50] We compared sugar yields from integrated processing of switchgrass (10 wt% loading) with pretreatment at different [Ch][Lys] concentrations (5–20 wt%) (Fig. S5, ESI†). Results show that, 74% glucose and 30% xylose yields are achieved using 10 wt% [Ch][Lys] as a pretreatment medium followed with the saccharification steps, which is comparable to values generated by pretreatment using 90 wt% [Ch][Lys] and subsequent dilution to 10 wt% for saccharification (Fig. 6a).

Equipped with: (1) a biocompatible IL from our screen on 15 ILs; (2) a viable method to overcome pH mismatch; and (3) reversibility of the process enabling IL reuse for continuous mode of operations, we set out to test our goal for conducting simultaneous saccharification and fermentation (SFF) using this new integrated configuration in order to produce ethanol using wild type *S. cerevisiae*. Fig. 4b highlight ethanol productivity of 0.139 g ethanol per gram of starting switchgrass, which translates to 83.3% of the theoretical ethanol yield from the initial levels of available glucan.

Mass balance, lignin fractionation and IL reuse

The mass flows of glucan, xylan, lignin, and ethanol were tracked in each of the streams coming in and out from the integrated consolidated processing of switchgrass using [Ch][Lys] and CO_2 (Fig. S6, ESI†). It is noted that only $\sim$9% of the glucan and 6% the xylan was intact in residual solids, confirming that most of the sugars have been released/utilized during pretreatment and SSF. Above 90% of the glucose in liquid stream is fermented to ethanol, xylose and xylose oligomers was remained in liquid stream because of the lack of pentose fermentation metabolism in wild-type yeast. However, both hexose and pentose sugars can be potentially co-fermented using microbes capable of fermenting both.[51,52] In the future, C5–C6 co-fermenting yeasts or other microbes capable of fermenting the majority of the sugars present simultaneously will be investigated that would increase the overall efficiency of the process. The majority of the lignin ($\sim$85%) was recovered in the residual solid streams.

In general, the strong interactions between a strong base like [Ch][Lys] and lignin could pose a problem for IL recycle and reuse. However this was not observed to be the case, since in our integrated approach the IL–lignin interactions were significantly weakened due to the pH drop from 12 to $\sim$7 by CO_2 absorption. Earlier studies have shown that hydrogen-bonding interactions between lignin and ILs were weakened or even eliminated by the addition of water.[53] Our theoretical study confirmed that the association of dilignol and [Ch][Lys] gradually decreased during progressive addition of water molecules (Fig. 5a). Since the molar ratio of H_2O to IL (250 : 1) is high in this integrated process, the strong interactions between lignin and IL tend to break down.

An added advantage of this CO_2 based integrated process is that separations are minimized as there are no post-processing steps between unit operations that are typically required. This integrated configuration also enables easy regeneration of the IL by simply elevating the temperature of the solution (*e.g.* from room temperature to 70 °C, Fig. 5b) or by bubbling with nitrogen gas (N_2), driving out the CO_2 and restoring the pH to its original value. Data points were collected until the feed reached its mass balance. Higher temperature required a shorter balanced time. The IL recovery for reuse included dehydrating the [Ch][Lys] to 10 wt% H_2O using vacuum distillation after lignin precipitation and filtration. Elemental analysis shows that the %N in the dry solid after fermentation was 1.96%. Considering untreated biomass contains N ($\sim$0.63%), the maximum [Ch][Lys]% in the residue was therefore calculated to be 0.65% as it is the only potential nitrogen source used in the process. The upper limit of [Ch][Lys] loss was therefore found to be 0.33%, and IL recovery obtained was above 99.67% conservatively and could be higher by condition optimization. The recycled IL performed very well as compared to neat IL, as indicated by the nearly identical ethanol yield after fermentation (Fig. 5c). In the current study we used vacuum distillation to demonstrate [Ch][Lys] dehydration and recycle, but we recognize that a more comprehensive study is warranted that includes other methods such as forward and reverse osmosis,[54] pervaporation and electrodialysis.[55] This integrated process provides a compelling example of a promising integrated biomass conversion technology, with the added advantage of facilitated IL recycle and lignin recovery.

Process intensification and technoeconomic analysis

In an order to examine the prospect of industrial implementation of this CO_2 based integrated biomass processing concept,

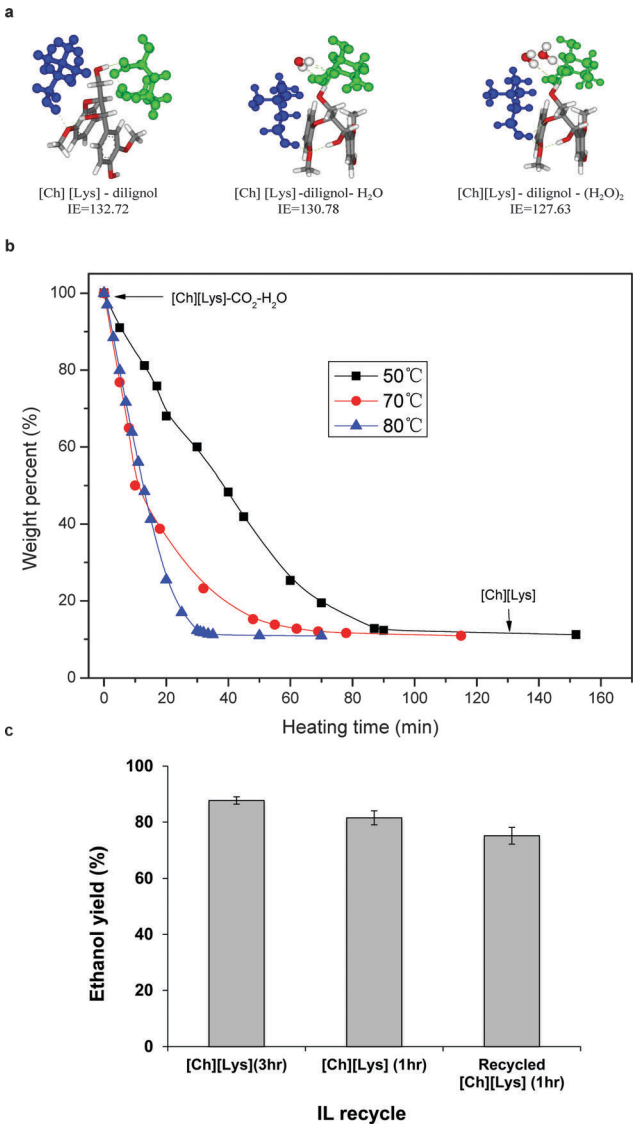

Fig. 5 Optimized geometries of dilignol and [Ch][Lys] complex in the presence of water molecules (a), effect of temperature on [Ch][Lys] regeneration after 10 wt% [Ch][Lys] aqueous system absorbed by CO_2 (b), and preliminary IL recycle performance on ethanol yield (c). In (a), interaction energy (IE) calculated at M06-2X/6-311++G(d,p) is reported in kcal mol^{-1}.

process intensification was carried out. We systematically increased the biomass loadings to 15, 20 and 30 wt% both for pretreatment and saccharification steps. The resulting glucose titers were approximately 32, 41 and 63 g L^{-1} respectively (Fig. S10, ESI†). Glucose titers were further improved by increasing the enzymes loading to 20 mg protein per gram of biomass. This increase of glucose titer was more pronounced for the higher loadings and had a minimum impact on low loading pretreatment and saccharification (10 wt% and below). Ethanol fermentation was carried out as described earlier. Results indicate that in our SSF process the highest ethanol titer of 25 g L^{-1} was observed for 20 wt% loadings at higher enzyme dose of 20 mg protein per gram of biomass. Although 30 wt% pretreatment and saccharifications loading resulted in highest sugar titer, the ethanol titer was observed to decrease. Both sugar titers at higher than 30 wt% loadings and ethanol titers at higher than 20 wt% loadings appear to be impacted due to poor mass transfer. An improved reactor design optimized for improved mixing would enhance mass transfer and should alleviate this problem. In addition, this process intensification data illustrates the upper limit of loadings for the pretreatment step. At loadings higher than 30 wt%, in addition to poor mass transfer, the pH adjustment utilizing CO_2 will pose problems, as there is not enough [Ch][Lys] and water to interact with CO_2 needed for the acidification.

We conducted a preliminary technoeconomic analysis (TEA) and sensitivity analysis to understand the advantages and challenges associated with the integrated CO_2 process demonstrated in this study. We analyzed two routes as benchmarks that have established TEA models in the scientific literature: the water-wash (WW) and JTherm processes.[18,56] The WW route is an IL pretreatment process that requires the removal of IL prior to the enzymatic hydrolysis so as not to inhibit enzyme activity and yeast growth. The JTherm process is our previously published process that eliminates the need for IL removal prior to hydrolysis with the use of the JTherm IL–tolerant enzyme mixture. More detailed information on our proposed route and the two benchmarks can be found in the Materials and methods section and the ESI† (Fig. S7–S9 and Table S3). We built integrated biorefinery models for each case using SuperPro Designer (a commercially available software package) that reflect industrial scale facilities with mature process technologies (*i.e.*, Nth plant), capable of processing 2000 dry MT per day of biomass. Consistent with studies published by the national renewable energy laboratory (NREL),[57] minimum ethanol selling price (MESP) is used as a benchmark for economic performance.

Our preliminary analysis indicates that the integrated CO_2 process has the potential to reduce the annual operating costs by around 50–65% compared to the WW and JTherm processes studied (Fig. S11, ESI†), although the sensitivity analysis presented in Fig. 6b highlights the importance of further research and scale-up activities to ensure high IL recovery rates. To identify specific cost drivers, a detailed section-wide breakdown of AOC is given (Fig. S12, ESI†). The JTherm process is particularly expensive due to the costs associated with the recovery of sugars from hydrolysate prior to fermentation. The integrated CO_2 process, in contrast, utilizes a biocompatible IL and thus no sugar extraction step is required prior to fermentation. Another factor contributing to the improved economics of the integrated CO_2 process is the use of aqueous IL mixtures at dilute [Ch][Lys] concentrations. The cumulative impact of reduced IL and water usage as well as the avoidance of intermediate separation steps makes the integrated CO_2 process an economically attractive route even when compared with the traditional WW route. This is evident from the lower pretreatment, wastewater treatment, and cogeneration/utility costs observed in the case of integrated CO_2 route (Fig. S12, ESI†). The projected MESP corresponding to the integrated CO_2

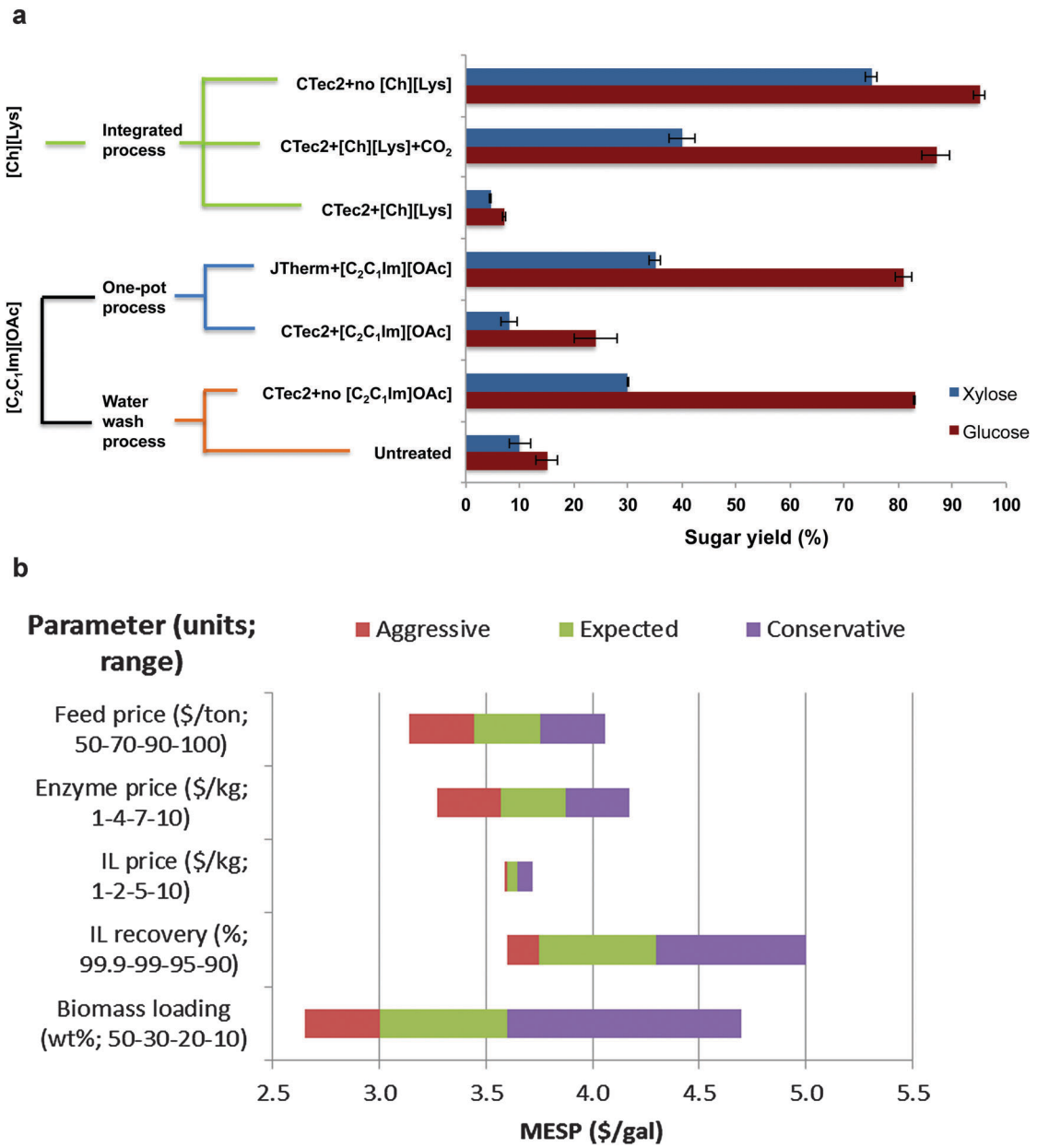

Fig. 6 Sugar yields for $[C_2C_1Im][OAc]$ (bottom) and [Ch][Lys] (top) obtained from conventional, integrated and CO_2 processes (a), and sensitivity analysis: variation in the MESP with potential variation in the key cost drivers (b). Conditions in (a): (a) water wash process, pretreatment (10 wt% SG, 90 wt% $[C_2C_1Im][OAc]$, 160 °C, 3 h), saccharification (2 wt% solid loading, 10 mg CTec2 + HTec2 per g raw SG, 50 mM citric buffer (pH 4.8), 50 °C, 72 h); (b) TEA sensitivity analysis for the proposed integrated CO_2 process.

route is less than $4 per gal, which represents a significant reduction compared to the WW route (with MESP around $7.2 per gal).

To understand the impact of potential variations in the key technical and economic parameters on the MESP, we have conducted a sensitivity analysis and results are presented in Fig. 6b. The sensitivity analysis includes IL price, fraction of IL recovered, enzyme price, feedstock price, and biomass loading. Included are three separate ranges for each key parameter: aggressive, expected, and conservative. The results indicate that both the feedstock and enzyme price have a significant impact on the MESP. Because of the high IL recovery (99.9%) assumed in the base case and the use of an aqueous rather than pure IL, the MESP is less sensitive to the IL price. Achieving this high recovery rate during scale-up presents a potential technical challenge. At lower IL recovery rates of 95% or less, the MESP would likely to be upwards of $4 per gal regardless of the price of IL (*i.e.*, even with $2 per kg IL). Biomass loading was also found to have a significant impact on the MESP and high biomass loadings (>30 wt%) can potentially bring the MESP to less than $3 per gal. Future advancements in lignin separation and utilization will enable us to conduct a more rigorous TEA,

and the production of high-value lignin-derived co-products will likely further reduce the projected MESP. Nonetheless, the preliminary TEA has helped to identify the potential opportunities and key cost drivers associated with this integrated CO_2 route as compared to previous IL conversion technologies.

Conclusions

We have demonstrated an innovative strategy to overcome some of the most significant challenges with IL-based pretreatment technologies by developing an integrated biomass conversion system that exploits chemistry between a biocompatible IL, [Ch][Lys], and CO_2 as a means of reversibly controlling pH and overcoming the problem of salt formation and IL loss. The IL recycling using this concept is demonstrated. The key advantages of this approach are: (1) integrated IL biomass pretreatment, saccharification and fermentation that does not require IL tolerant enzyme cocktails, several unit operations, or extensive water washes; (2) eliminates the addition of mineral acids/organic acids and salt accumulation thus making the recycle of IL much easier and viable; (3) allows for 87% glucose and over 40% xylose (monomers) yields during saccharification using a commercial enzyme mixture; (4) enables direct fermentation of sugars from biomass to 83.3% of the theoretical ethanol yield from glucose using wild type *S. cerevisiae* fermentation host; (5) high ethanol titer achieved by high biomass loading; and (6) facilitates lignin separation and reduced IL loss. Our preliminary TEA indicated that this integrated approach has the potential to significantly reduce biofuel production cost. Our strategy thus opens up new avenues for developing environmentally sustainable, scalable, and cost-effective integrated IL conversion technologies for the production of fermentable sugars, biofuels, renewable chemicals, and other co-products derived from non-food sustainable lignocellulosic biomass.

Materials and methods

Materials

Switchgrass (*Panicum virgatum*) provided by Dr Daniel Putnam, University of California at Davis was ground to 20–40 mesh by a Wiley Mill through a 2 mm screen and fractionated by a vibratory sieve system (Endecotts, Ponte Vedra, FL). The switchgrass contains 29.6% cellulose, 18.4% xylan, 20.0% lignin, 8.1% moisture and 23.9% of other compounds remaining unidentified, on wet basis.[19] Microcrystalline cellulose (Avicel) was purchased from Sigma-Aldrich (St. Louis, MO). [C_2C_1Im][OAc], was purchased from BASF (lot no. 08-0010, purity >95%, Basionics™ BC-01, Florham Park, NJ). The other imidazolium based ILs were purchased from IoLiTec ILa Technologies Inc (Tuscsaloosa, AL). [Ch][Lys] was synthesized according to the literature,[58] and used after dried under vacuum. The commercial enzyme products cellulase (Cellic®CTec2, Batch#VCN10001) and hemicellulase (Cellic®HTec2, Batch#VHN00001) were gifts from Novozymes (Franklinton, NC).

Compositional analysis

Compositional analysis of switchgrass was described in our previous work,[34] the data of the pretreated switchgrass using [ChLys] under different conditions were provided in Table S2, ESI.†

Integrated pretreatment and saccharification. In an integrated process shown in Fig. 4, switchgrass (100 mg) was mixed with [Ch][Lys] (900 mg) at a 10 wt% biomass loading in a 15 mL capped glass pressure tube (Ace Glass) and pretreated in an oil bath at 140 °C for 1 h. Untreated raw switchgrass (30–40 mesh) was used as a control. After pretreatment, the slurry was diluted with water to obtain a final IL concentration of 5, 10 or 20 wt%. Before and after the addition of enzyme mixture (CTec2/HTec2 = 9 : 1, v/v) for the saccharification, a 1 MPa pressure of CO_2 was applied to the reactor to drop and maintain the pH of the system as detailed in the following section. Enzymatic hydrolysis was conducted at 50 °C, with constant agitation on an Enviro Genie SI-1200 rotator platform (Scientific Industries, Inc., Bohemia, Ny). For comparisons, no pH adjustment and no IL saccharification processes were carried out after pretreatment, respectively. The pretreated biomass was washed 6 times with hot water to remove residual ILs and soluble sugars. Washed IL pretreated solids were dried by lyophilization, weighed and resuspended with water or buffer solution before adding the enzyme cocktail. In another set of integrated processes shown in Fig. S4, ESI,† switchgrass (100 mg) was mixed with water and 50, 100, or 200 mg [Ch][Lys] at a 10 wt% biomass loading in a 15 mL capped glass pressure tube and pretreated at 140 °C for 1 h. After pretreatment, enzyme mixture (9 : 1 v/v) was directly added to the slurry at 10 mg EP per g starting biomass for saccharification at the same conditions as stated above.

CO_2-based pH adjustment

All the CO_2 absorption experiments were carried out at room temperature in a 25 mL stainless steel Parr reactor (Parr instrument Co., USA) equipped with a magnetic stirrer plate and CO_2 cylinder (>99.9% CO_2 purity). In a typical procedure, 10 mL a certain concentration of [Ch][Lys] aqueous system was added into the Parr. After being sealed, the Parr was stirred at room temperature, and the absorption pressure was held constant by a backpressure valve. After the absorption was completed, the remaining CO_2 was removed slowly from the Parr. Then, the corresponding pH value of the mixture was quickly analyzed by Orion™ 3-Star Benchtop pH Meter. To elucidate the interaction between CO_2 with side amine and terminal amine groups of [Ch][Lys] in H_2O, we conducted ^{13}C nuclear magnetic resonance (NMR) (Bruker Avance-600 MHz, DMSO-d_6) analysis of [Ch][Lys] before and after CO_2 absorption.

Simultaneous saccharification and fermentation

As an example, yeast (*Saccharomyces cerevisiae*) strain BY4741 (MATa his3Δ0 leu2Δ0 met15Δ0 ura3Δ0, a derivative of S288C) was propagated in liquid YPD media for 24 h. The cells were recovered by centrifugation at 3220 rcf for 5 min and washed three times by 0.2% sterile peptone solution. Switchgrass (600 mg) was mixed with [Ch][Lys] (600 mg) and water (4.8 g)

at a 10 wt% biomass loading in a 15 mL capped glass pressure tube and pretreated at 140 °C for 1 or 3 h. After pretreatment, the slurry was diluted with 6 mL water and CTec2 + HTec2 (9 : 1 v/v) mixture was then added at 10 mg EP per g starting biomass. The mixture was carbonated under 1 MPa CO_2 pressure and incubated at 50 °C for 18 h for saccharification and then cooled down to 37 °C for yeast inoculation to a concentration of 5 g L^{-1} yeast cells (based on dry weight). After 72 h of SSF, the fermentation broth was chilled on ice and centrifuged to separate the solid and liquid. After fermentation, lignin was separated by centrifugation and washed three times with DI water to minimize the IL residue. All of the liquid streams were combined together and concentrated to a half volume of the fermentation system (*e.g.* 12 mL) by using vacuum distillation at 50 °C. During this process, the IL was dehydrated from 5 wt% to around 10 wt% and used for the next run.

Theoretical computation

All of the calculations were performed with the Gaussian 09 software package. The geometries of all of the [Ch][Lys] IL, CO_2 mediated IL complexes, were fully optimized at the M06-2X/6-311++G(d,p) level of theory. The stable structures were verified by analyzing the corresponding geometries obtained from our calculations and interaction energies (IEs) were corrected for basis set superposition error. In the present study, acidity values were calculated using the DFT based global reactivity descriptors,[28] such as chemical hardness and chemical potential[59] of the IL–H_2O–CO_2 complexes. Natural bond orbital analyses were performed to determine the atomic charges and local nucleophilicity values[60] were derived.

Technoeconomic analysis

To facilitate the preliminary TEA conducted in this study, process models for all the three configurations (WW, JTherm, and integrated CO_2) were built in SuperPro Designer. Each biorefinery model consists of multiple sections including feed handling, pretreatment and hydrolysis, fermentation, product recovery, wastewater treatment (WWT) and on-site cogeneration facility. However, each of these three configurations is characteristically different from one another (see Fig. S7–S9, ESI†). For instance, the WW route requires that the IL to be removed prior to hydrolysis, in which case the remainder of the process is very similar to biorefineries utilizing dilute acid pretreatment.[57] Conversely, the integrated configurations do not require the IL to be removed prior to the hydrolysis-this is due to the use of IL–tolerant enzymes (*i.e.*, JTherm route) or biocompatible IL (*i.e.*, integrated CO_2 route). In the case of JTherm route, sugars must be extracted from the hydrolysate, which was accomplished using liquid–liquid extraction (LLE) technique as discussed in our previous work.[56] In contrast to the JTherm route, the integrated CO_2 process' use of a biocompatible IL allows for simultaneous saccharification and fermentation (SSF) in the presence of IL. The configurations for the WW and JTherm routes are based on our previous work,[56] while the process configuration for the integrated CO_2 is original to this study. Key parameters used in the TEA are given (Table S3, ESI†).

Consistent with a recent study from NREL,[57] our study is based on an assumed Nth plant, in which some parameters are based on presumed improvements in mature, industrial-scale facilities. First, industrially relevant biomass loading (20%) was assumed during pretreatment in all the three routes. In addition, high glucan/xylan conversion in hydrolysis (90%) and high glucose/xylose conversion in fermentation (90%) were used. All the costs and efficiencies of processing steps (including IL recovery, downstream, *etc.*) are based on future, mature technologies. For instance, we modeled IL recovery using pervaporation with a high IL recovery (~99.9%) for all routes; furthermore, 50% of the pervaporation feed heating need is assumed to be met by recovering heat from the condensing permeate stream. Since the main scope of this study is related to the upstream sections (*i.e.*, pretreatment, hydrolysis, fermentation), the downstream operations (*e.g.*, product recovery, any intermediate separations such as water-wash, sugar extraction) were optimized consistently in all the three routes. Wastewater generated in the process was treated in wastewater treatment (WWT) section that consists of primarily anaerobic and aerobic digesters. Because of the high IL recovery rate, any impact of the residual IL on the WWT section is assumed to be negligible. The economic analysis was based on the method suggested by NREL[57] and Minimum Ethanol Selling Price (MESP) was used as the economic metric. The MESP is computed through a detailed cash flow analysis with an Internal Rate of Return (IRR) of 10%. The base year in the economic analysis is 2014.

Author contributions

SS and JS conceptualized and designed the experiment. JS, JS, TD and FX performed experiments. RP performed theoretical computation. MK and CS did technoeconomic analysis. All authors contributed to data analysis, experimental design and manuscript writing.

Author information

The authors declare no competing financial interests. Readers are welcome to comment on the online version of the paper. Correspondence and requests for materials should be addressed to S. S. (seesing@sandia.gov).

Acknowledgements

This work conducted by the Joint BioEnergy Institute was supported by the Office of Science, Office of Biological and Environmental Research of the U.S. Department of Energy under contract no. DE-AC02-05CH11231. The enzymes used in this manuscript were provided by Novozymes. The authors thank Britt Abrahamson, Dr Ning Sun and Dr Douglas Higgins for assistance in IL toxicity screening experiments and Nathan Hillson for assistance in reviewing the manuscript.

References

1 C. Schubert, *Nat. Biotechnol.*, 2006, **24**, 777–784.
2 C. Somerville, H. Youngs, C. Taylor, S. C. Davis and S. P. Long, *Science*, 2010, **329**, 790–792.
3 I. Gelfand, R. Sahajpal, X. Zhang, R. C. Izaurralde, K. L. Gross and G. P. Robertson, *Nature*, 2013, **493**, 514–517.
4 M. E. Himmel, S. Y. Ding, D. K. Johnson, W. S. Adney, M. R. Nimlos, J. W. Brady and T. D. Foust, *Science*, 2007, **315**, 804–807.
5 S. Singh and B. A. Simmons, *Aqueous Pretreatment of Plant Biomass for Biological and Chemical Conversion to Fuels and Chemicals*, John Wiley & Sons, Ltd, 2013, pp. 223–238, ch. 11, DOI: 10.1002/9780470975831.
6 B. Yang and C. E. Wyman, *Biofuels, Bioprod. Biorefin.*, 2008, **2**, 26–40.
7 T. Dutta, J. Shi, J. Sun, X. Zhang, G. Cheng, B. A. Simmons and S. Singh, *Ionic Liquids in the Biorefinery Concept: Challenges and Perspectives*, 2015, vol. 65.
8 C. Li, L. Sun, B. Simmons and S. Singh, *BioEnergy Res.*, 2013, **6**, 14–23.
9 S. Singh, B. A. Simmons and K. P. Vogel, *Biotechnol. Bioeng.*, 2009, **104**, 68–75.
10 P. Alvira, E. Tomas-Pejo, M. Ballesteros and M. J. Negro, *Bioresour. Technol.*, 2010, **101**, 4851–4861.
11 P. Varanasi, P. Singh, M. Auer, P. D. Adams, B. A. Simmons and S. Singh, *Biotechnol. Biofuels*, 2013, **6**, 1–9.
12 J. Shi, V. S. Thompson, N. A. Yancey, V. Stavila, B. A. Simmons and S. Singh, *Biofuels*, 2013, **4**, 63–72.
13 A. G. Cruz, C. Scullin, C. Mu, G. Cheng, V. Stavila, P. Varanasi, D. Y. Xu, J. Mentel, Y. D. Chuang, B. A. Simmons and S. Singh, *Biotechnol. Biofuels*, 2013, **6**, 1–9.
14 C. L. Li, D. Tanjore, W. He, J. Wong, J. L. Gardner, K. L. Sale, B. A. Simmons and S. Singh, *Biotechnol. Biofuels*, 2013, **6**, 1–13.
15 A. S. A. da Silva, R. S. S. Teixeira, T. Endo, E. P. S. Bon and S.-H. Lee, *Green Chem.*, 2013, **15**, 1991–2001.
16 S. Datta, B. Holmes, J. I. Park, Z. W. Chen, D. C. Dibble, M. Hadi, H. W. Blanch, B. A. Simmons and R. Sapra, *Green Chem.*, 2010, **12**, 338–345.
17 J. M. Gladden, J. I. Park, J. Bergmann, V. Reyes-Ortiz, P. D'haeseleer, B. F. Quirino, K. L. Sale, B. A. Simmons and S. W. Singer, *Biotechnol. Biofuels*, 2014, **7**, 1–12.
18 D. Klein-Marcuschamer, B. A. Simmons and H. W. Blanch, *Biofuels, Bioprod. Biorefin.*, 2011, **5**, 562–569.
19 J. Shi, J. M. Gladden, N. Sathitsuksanoh, P. Kambam, L. Sandoval, D. Mitra, S. Zhang, A. George, S. W. Singer, B. A. Simmons and S. Singh, *Green Chem.*, 2013, **15**, 2579–2589.
20 M. Ouellet, S. Datta, D. C. Dibble, P. R. Tamrakar, P. I. Benke, C. Li, S. Singh, K. L. Sale, P. D. Adams, J. D. Keasling, B. A. Simmons, B. M. Holmes and A. Mukhopadhyay, *Green Chem.*, 2011, **13**, 2743–2749.
21 T. L. Ruegg, E.-M. Kim, B. A. Simmons, J. D. Keasling, S. W. Singer, T. Soon Lee and M. P. Thelen, *Nat. Commun.*, 2014, **5**.
22 I. R. Sitepu, S. Shi, B. A. Simmons, S. W. Singer, K. Boundy-Mills and C. W. Simmons, *FEMS Yeast Res.*, 2014, **14**, 1286–1294.
23 L. S. Parreiras, R. J. Breuer, R. Avanasi Narasimhan, A. J. Higbee, A. La Reau, M. Tremaine, L. Qin, L. B. Willis, B. D. Bice, B. L. Bonfert, R. C. Pinhancos, A. J. Balloon, N. Uppugundla, T. Liu, C. Li, D. Tanjore, I. M. Ong, H. Li, E. L. Pohlmann, J. Serate, S. T. Withers, B. A. Simmons, D. B. Hodge, M. S. Westphall, J. J. Coon, B. E. Dale, V. Balan, D. H. Keating, Y. Zhang, R. Landick, A. P. Gasch and T. K. Sato, *PLoS One*, 2014, **9**, e107499.
24 K. Ninomiya, T. Yamauchi, M. Kobayashi, C. Ogino, N. Shimizu and K. Takahashi, *Biochem. Eng. J.*, 2013, **71**, 25–29.
25 K. Ohira, Y. Abe, M. Kawatsura, K. Suzuki, M. Mizuno, Y. Amano and T. Itoh, *ChemSusChem*, 2012, **5**, 388–391.
26 X.-D. Hou, Q.-P. Liu, T. J. Smith, N. Li and M.-H. Zong, *PLoS One*, 2013, **8**, e59145.
27 L. C. Tomé, D. J. S. Patinha, R. Ferreira, H. Garcia, C. Silva Pereira, C. S. R. Freire, L. P. N. Rebelo and I. M. Marrucho, *ChemSusChem*, 2014, **7**, 110–113.
28 A. M. Socha, R. Parthasarathi, J. Shi, S. Pattathil, D. Whyte, M. Bergeron, A. George, K. Tran, V. Stavila, S. Venkatachalam, M. G. Hahn, B. A. Simmons and S. Singh, *Proc. Natl. Acad. Sci. U. S. A.*, 2014, **111**, E3587–E3595.
29 F. Xu, J. Sun, N. V. S. N. M. Konda, J. Shi, T. Dutta, C. D. Scown, B. A. Simmons and S. Singh, *Energy Environ. Sci.*, 2016, **9**, 1042–1049.
30 R. Kajaste, *J. Cleaner Prod.*, 2014, **75**, 1–10.
31 L. C. Tome, D. J. S. Patinha, R. Ferreira, H. Garcia, C. S. Pereira, C. S. R. Freire, L. P. N. Rebelo and I. M. Marrucho, *ChemSusChem*, 2014, **7**, 110–113.
32 J. Zhang, S. Zhang, K. Dong, Y. Zhang, Y. Shen and X. Lv, *Chem. – Eur. J.*, 2006, **12**, 4021–4026.
33 Y. Zhang, S. Zhang, X. Lu, Q. Zhou, W. Fan and X. Zhang, *Chem. – Eur. J.*, 2009, **15**, 3003–3011.
34 N. Sun, R. Parthasarathi, A. M. Socha, J. Shi, S. Zhang, V. Stavila, K. L. Sale, B. A. Simmons and S. Singh, *Green Chem.*, 2014, **16**, 2546–2557.
35 T. V. Doherty, M. Mora-Pale, S. E. Foley, R. J. Linhardt and J. S. Dordick, *Green Chem.*, 2010, **12**, 1967–1975.
36 Y. Fukaya, K. Hayashi, M. Wada and H. Ohno, *Green Chem.*, 2008, **10**, 44–46.
37 R. P. Swatloski, S. K. Spear, J. D. Holbrey and R. D. Rogers, *J. Am. Chem. Soc.*, 2002, **124**, 4974–4975.
38 G. Cheng, X. Zhang, B. Simmons and S. Singh, *Energy Environ. Sci.*, 2015, **8**, 436–455.
39 X. D. Gao, R. Kumar, S. Singh, B. A. Simmons, V. Balan, B. E. Dale and C. E. Wyman, *Biotechnol. Biofuels*, 2014, **7**, 1–13.
40 N. Uppugundla, L. D. Sousa, S. P. S. Chundawat, X. R. Yu, B. Simmons, S. Singh, X. D. Gao, R. Kumar, C. E. Wyman, B. E. Dale and V. Balan, *Biotechnol. Biofuels*, 2014, **7**, 1–14.
41 B. Simmons, S. Singh, B. M. Holmes and H. W. Blanch, *Chem. Eng. Prog.*, 2012, vol. 106, pp. 50–55.
42 C. A. Ober and R. B. Gupta, *Ind. Eng. Chem. Res.*, 2012, **51**, 2524–2530.

43 M. Pera-Titus, *Chem. Rev.*, 2013, **114**, 1413–1492.
44 G. T. Rochelle, *Science*, 2009, **325**, 1652–1654.
45 H. Yamada, Y. Matsuzaki, T. Higashii and S. Kazama, *J. Phys. Chem. A*, 2011, **115**, 3079–3086.
46 G. Elert and S. Meraj, *The Physics Factbook*, 2000.
47 G. Giaever, A. M. Chu, L. Ni, C. Connelly, L. Riles, S. Veronneau, S. Dow, A. Lucau-Danila, K. Anderson, B. Andre, A. P. Arkin, A. Astromoff, M. El Bakkoury, R. Bangham, R. Benito, S. Brachat, S. Campanaro, M. Curtiss, K. Davis, A. Deutschbauer, K. D. Entian, P. Flaherty, F. Foury, D. J. Garfinkel, M. Gerstein, D. Gotte, U. Guldener, J. H. Hegemann, S. Hempel, Z. Herman, D. F. Jaramillo, D. E. Kelly, S. L. Kelly, P. Kotter, D. LaBonte, D. C. Lamb, N. Lan, H. Liang, H. Liao, L. Liu, C. Y. Luo, M. Lussier, R. Mao, P. Menard, S. L. Ooi, J. L. Revuelta, C. J. Roberts, M. Rose, P. Ross-Macdonald, B. Scherens, G. Schimmack, B. Shafer, D. D. Shoemaker, S. Sookhai-Mahadeo, R. K. Storms, J. N. Strathern, G. Valle, M. Voet, G. Volckaert, C. Y. Wang, T. R. Ward, J. Wilhelmy, E. A. Winzeler, Y. H. Yang, G. Yen, E. Youngman, K. X. Yu, H. Bussey, J. D. Boeke, M. Snyder, P. Philippsen, R. W. Davis and M. Johnston, *Nature*, 2002, **418**, 387–391.
48 R. Serrano, D. Bernal, E. Simon and J. Arino, *J. Biol. Chem.*, 2004, **279**, 19698–19704.
49 R. Serrano, H. Martin, A. Casamayor and J. Arino, *J. Biol. Chem.*, 2006, **281**, 39785–39795.
50 J. Shi, K. Balamurugan, R. Parthasarathi, N. Sathitsuksanoh, S. Zhang, V. Stavila, V. Subramanian, B. A. Simmons and S. Singh, *Green Chem.*, 2014, **16**, 3830–3840.
51 M. Zhang, C. Eddy, K. Deanda, M. Finkelstein and S. Picataggio, *Science*, 1995, **267**, 240–243.
52 M. W. Lau and B. E. Dale, *Proc. Natl. Acad. Sci. U. S. A.*, 2009, **106**, 1368–1373.
53 W. Y. Ji, Z. D. Ding, J. H. Liu, Q. X. Song, X. L. Xia, H. Y. Gao, H. J. Wang and W. X. Gu, *Energy Fuels*, 2012, **26**, 6393–6403.
54 H. Meng, B. B. Gong, T. Geng and C. X. Li, *Appl. Surf. Sci.*, 2014, **292**, 638–644.
55 X. L. Wang, Y. Nie, X. P. Zhang, S. J. Zhang and J. W. Li, *Desalination*, 2012, **285**, 205–212.
56 N. V. S. N. M. Konda, J. Shi, S. Singh, H. W. Blanch, B. A. Simmons and D. Klein-Marcuschamer, *Biotechnol. Biofuels*, 2014, **7**, 86.
57 D. Humbird, R. Davis, L. Tao, C. Kinchin, D. Hsu, D. David, A. Aden, *National Renewable Energy Technology*, 2011, vol. 275, p. 3000.
58 Q. P. Liu, X. D. Hou, N. Li and M. H. Zong, *Green Chem.*, 2012, **14**, 304–307.
59 R. G. Parr and R. G. P. W. Yang, *Density-functional theory of atoms and molecules*, Oxford University Press, 1989.
60 R. Parthasarathi, J. Padmanabhan, M. Elango, V. Subramanian and P. Chattaraj, *Chem. Phys. Lett.*, 2004, **394**, 225–230.